AGU PUBLICATIONS

JGR

Journal of Geophysical Research: Oceans

RESEARCH ARTICLE

10.1002/2014JC010516

Key Points:
- XBTs from the Oleander line provide a 37 year record of MAB shelf temperatures
- Recent Middle Atlantic Bight warming is concentrated near the shelfbreak front
- MAB shelf temperature anomalies lag coastal sea level anomalies by 2 years

Correspondence to:
M. Andres,
mandres@whoi.edu

Citation:
Forsyth, J. S. T., M. Andres, and G. G. Gawarkiewicz (2015), Recent accelerated warming of the continental shelf off New Jersey: Observations from the CMV Oleander expendable bathythermograph line, *J. Geophys. Res. Oceans*, *120*, 2370–2384, doi:10.1002/2014JC010516.

Received 20 OCT 2014
Accepted 25 FEB 2015
Accepted article online 2 MAR 2015
Published online 27 MAR 2015
Corrected 24 APR 2015

This article was corrected on 24 APR 2015. See the end of the full text for details.

Recent accelerated warming of the continental shelf off New Jersey: Observations from the CMV Oleander expendable bathythermograph line

Jacob Samuel Tse Forsyth[1,2], Magdalena Andres[2], and Glen G. Gawarkiewicz[2]

[1]Department of Physics and Astronomy and Department of Economics, Bowdoin College, Brunswick, Maine, USA, [2]Department of Physical Oceanography, Woods Hole Oceanographic Institution, Woods Hole, Massachusetts, USA

Abstract Expendable bathythermographs (XBTs) have been launched along a repeat track from New Jersey to Bermuda from the CMV Oleander through the NOAA/NEFSC Ship of Opportunity Program about 14 times per year since 1977. The XBT temperatures on the Middle Atlantic Bight shelf are binned with 10 km horizontal and 5 m vertical resolution to produce monthly, seasonally, and annually averaged cross-shelf temperature sections. The depth-averaged shelf temperature, T_s, calculated from annually averaged sections that are spatially averaged across the shelf, increases at $0.026 \pm 0.001^{\circ}$C yr^{-1} from 1977 to 2013, with the recent trend substantially larger than the overall 37 year trend ($0.11 \pm 0.02^{\circ}$C yr^{-1} since 2002). The Oleander temperature sections suggest that the recent acceleration in warming on the shelf is not confined to the surface, but occurs throughout the water column with some contribution from interactions between the shelf and the adjacent Slope Sea reflected in cross-shelf motions of the shelfbreak front. The local warming on the shelf cannot explain the region's amplified rate of sea level rise relative to the global mean. Additionally, T_s exhibits significant interannual variability with the warmest anomalies increasing in intensity over the 37 year record even as the cold anomalies remain relatively uniform throughout the record. T_s anomalies are not correlated with annually averaged coastal sea level anomalies at zero lag. However, positive correlation is found between 2 year lagged T_s anomalies and coastal sea level anomalies, suggesting that the region's sea level anomalies may serve as a predictor of shelf temperature.

1. Introduction

Despite the observational evidence that ocean heat content (OHC) is increasing in the open ocean [*Abraham et al.*, 2013], changes over the continental shelves are difficult to quantify as many long-term ocean temperature records lack the horizontal, vertical, and temporal scales required to adequately resolve shelf variability. Though the global Argo program has greatly improved our ability to measure the temperature profiles in the open ocean and to monitor changes in OHC over the most recent decade [*Abraham et al.*, 2013], these floats, whose parking depth is 1000 m, cannot sample the shelves which are typically less than 100 m deep.

Here we present results from a remarkable data set of expendable bathymograph (XBT) temperature profiles, collected over 37 years (1977–2013) from the CMV Oleander along a repeat transect crossing the Middle Atlantic Bight (MAB) shelf. These data provide a means to examine the region's changing environment and the links between the sea level, the shelf temperature structure, and the shelf circulation. This data set is of regional interest both because of the northwestern North Atlantic's accelerated rate of sea level rise relative to the global mean [*Sallenger et al.*, 2012] and the area's collapsing fisheries [*Frank et al.*, 2005]. In addition, this long time series of temperature structure on the MAB shelf can provide insight into more general questions concerning the causes and consequences of open-ocean/shelf interactions in a region near the two major limbs of the Atlantic meridional overturning circulation (AMOC): the Gulf Stream and deep western boundary current (DWBC).

Increases in OHC lead to a rising mean sea level associated with the thermal expansion of seawater. Over the satellite altimetry period (i.e., 1993–2010), the observed global mean rate of sea level rise is 3.2 ± 0.4 mm yr^{-1} [*Church and White*, 2011] and the steric rise due to thermal expansion is estimated as $\sim$1/3 of this total rate [*Stammer et al.*, 2013]. Rates of sea level rise, however, are not spatially uniform [*Merrifield et al.*, 2009]. Since shelves are shallow, changes in the vertical temperature profiles on the shelf can

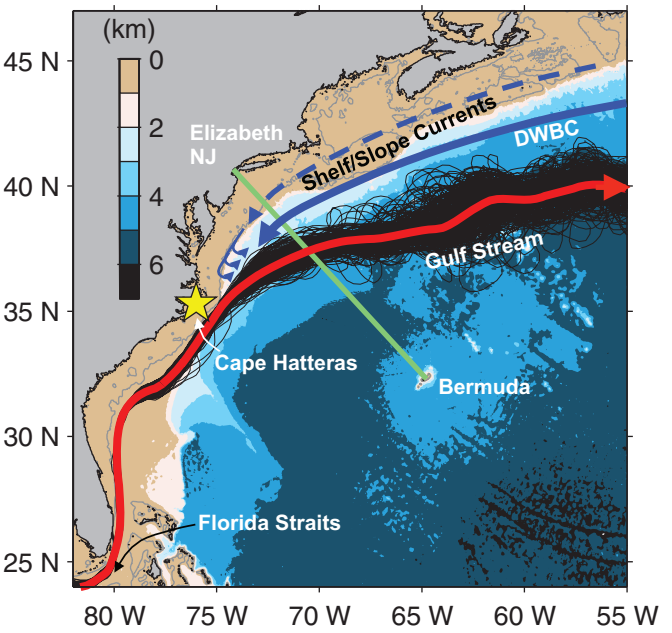

Figure 1. Schematic of the mean surface circulation in the northwestern North Atlantic. Oleander route (green), 200 m isobath (gray), and Gulf Stream meander envelope as indicated by the 40 cm contours (black) from monthly mean Aviso absolute dynamic topography maps are shown. Small blue arrows indicate "Ford" waters peeling off the shelf and becoming entrained in the Gulf Stream [*Ford et al.*, 1952].

have only a small influence on the global ocean heat budget. Also, any local changes in the steric sea level ΔSSH_{st} due to local temperature changes on the shelves must be modest:

$$\Delta SSH_{st} = \int_{-D}^{0} \alpha(T(z) - T_{ref})dz, \quad (1)$$

in which D is the water depth, α is the thermal expansion coefficient, $T(z)$ is the temperature profile and T_{ref} is a reference temperature profile. On the shelves, particularly near the coasts where the steric effect approaches zero as D decreases, differences between the regional sea level rise and the global mean rise may be associated with changes in the dynamic sea level that arise from changes in the circulation.

In the following, section 2 provides an overview of the mean circulation in the northwestern North Atlantic and discusses the temperature and sea level changes in the region comprising the MAB, Gulf of Maine, and Scotian Shelf. The data sets and the methodology used to generate monthly, seasonally, and annually averaged MAB shelf temperature cross sections from individual Oleander XBT transects are described in section 3. In section 4, the climatology generated from the Oleander data is compared with previous studies of the MAB shelf to demonstrate the quality of the XBT data set and to describe some of the salient features of MAB shelf processes. In addition, section 4 discusses the time series of the Oleander XBT-derived area-averaged shelf temperature (proportional to the shelf heat content). Section 5 discusses the shelf's interannual temperature variability and long-term trends, and compares these with other records in the region. Results are summarized in section 6 and implications for predictability on the MAB shelf are discussed.

2. The Northwestern North Atlantic

The dominant feature of the surface circulation in the western North Atlantic (Figure 1) is the Gulf Stream, which carries warm waters poleward in the warm upper limb of the AMOC. Between Florida Straits and Cape Hatteras, North Carolina, the current is a true western boundary current tightly constrained by the steep topography of the continental slope to flow near the shelfbreak. Flow over the South Atlantic Bight shelf (between Florida and Cape Hatteras) is generally in the same direction as that in the Gulf Stream, though with significantly weaker currents [*Savidge and Bane*, 2001]. Near Cape Hatteras, the Gulf Stream leaves the shelfbreak and transitions from a western boundary current to a vigorously meandering free jet after crossing over the DWBC, which carries cold, fresh waters equatorward in the AMOC's cold deeper limb [*Toole et al.*, 2011; *Peña-Molino and Joyce*, 2008]. Although the mean Gulf Stream path downstream of Cape Hatteras is separated from the MAB and Gulf of Maine shelves by the Slope Sea, pinched-off anticyclonic Gulf Stream rings [*Ramp et al.*, 1983; *Joyce et al.*, 1992; *Gawarkiewicz et al.*, 2001] and (very occasionally) large Gulf Stream path diversions [*Gawarkiewicz et al.*, 2012] do sometimes deliver the warm, subtropical Gulf Stream waters to the edge of the continental shelf.

On its approach toward Cape Hatteras and the Gulf Stream separation point, the southwestward-flowing DWBC follows the continental slope flowing between 2000 m and 4000 m isobaths onshore of the meandering Gulf Stream [*Joyce et al.*, 2005]. The DWBC here is relatively barotropic and exists as a weak surface-

to-bottom current (e.g., see 4 year Eulerian mean in *Toole et al*. [2011, Figure 3]) before passing under the Gulf Stream near Cape Hatteras [*Pickart and Watts*, 1990]. Further onshore, along the MAB and Gulf of Maine shelfbreak, a density front between the cooler, fresher shelf waters and the warmer, saltier Slope Sea waters supports the equatorward-flowing Shelfbreak jet [*Flagg et al*., 2006; *Gawarkiewicz et al*., 2008]. This is part of the larger shelfbreak current system of coastal circulations between Greenland and the southern MAB [*Fratantoni and Pickart*, 2007]. Mean along-shelf flows over the Gulf of Maine and MAB shelf are also equatorward – notably against the mean wind stress, suggesting a mean along-shelf pressure gradient force [*Lentz*, 2008]. Cold, fresh waters from the equatorward-flowing MAB shelf and slope currents are entrained into the cyclonic side of the Gulf Stream as "Ford" waters [*Churchill and Gawarkiewicz*, 2012; *Gawarkiewicz et al*., 2008; *Csanady and Hamilton*, 1988; *Gawarkiewicz and Linder*, 2006; *Ford et al*., 1952].

2.1. Changes on the Shelves: Trends and Interannual Variability

Ocean surface temperatures have been trending upward for the past 120 years in the MAB, at a rate of $0.007 \pm 0.003^{\circ}\mathrm{C\ yr^{-1}}$, and in the Gulf of Maine, at around $0.010 \pm 0.003^{\circ}\mathrm{C\ yr^{-1}}$ [*Shearman and Lentz*, 2010]. However, recent evidence suggests that over the past 30 years, the sea surface temperatures in the Gulf of Maine have increased more rapidly at $0.026^{\circ}\mathrm{C\ yr^{-1}}$ with the warming trend between 2004 and 2012 reportedly reaching $0.26^{\circ}\mathrm{C\ yr^{-1}}$ [*Mills et al*., 2013].

Sea level is also rising along the coast from Cape Hatteras to Nova Scotia and the rate is higher than the global mean rate of sea level rise. Furthermore, as noted above for the region's surface temperature trends, the rate of sea level rise here is apparently increasing [*Sallenger et al*., 2012]. Mechanisms underlying the amplified rate of sea level rise observed along the coast and over the shelves here are currently under debate. Initial studies attributed the accelerated rise to a slowing Gulf Stream and changes in the North Atlantic Oscillation (NAO) [*Ezer et al*., 2013]. However, observational evidence from Oleander ADCP measurements indicates the Gulf Stream transport is not significantly changing [*Rossby et al*., 2014] and therefore is not significantly contributing to the increase in sea level rise.

In addition to these long-term surface temperature and sea level trends in the coastal ocean off the northeastern United States and Canada, the shelves between Cape Hatteras and Nova Scotia exhibit strong interannual variability. In 2012, for example, the shelf's winter and spring water temperatures were among the warmest on record [*Mills et al*., 2013]. This has been attributed to anomalously low fall (2011) and wintertime (2012) heat exchange between the ocean and overlying atmosphere related to a northward shifted jet stream and greatly reduced heat loss from the ocean to the atmosphere during the winter [*Chen et al*., 2014]. While the region's 1970–2012 sea level trend is associated with a 160 mm net increase in coastal sea level, year-to-year changes in annually averaged coastal sea level ($\pm$50 mm) represent a significant fraction (about 2/3) of this total rise [*Andres et al*., 2013]. A proposed driver of interannual variations in sea level along the coast and over the shelves between Cape Hatteras and Nova Scotia is the region's along-shelf wind stress, which is highly correlated with interannual variability in sea level [*Andres et al*., 2013; *Li et al*., 2014].

3. Data sets and Methodology

3.1. Repeat XBT Line

Since 1977, XBTs have been launched regularly from the CMV Oleander, a container ship operated by Bermuda Container Lines, which traverses weekly between Elizabeth, New Jersey, and Bermuda (Figure 2). Through 2013, the data were collected as part of NOAA's Northeast Fisheries Science Center (NOAA/NEFSC) Ship of Opportunity Program (SOOP). The NOAA/NEFSC Program was cancelled in December 2013 and in mid-2014 the XBT data collection shifted to the National Science Foundation-sponsored Oleander Project, a companion effort that uses hull-mounted ADCPs to record upper-ocean velocities during the CMV Oleander crossings [*Flagg et al*., 1998; *Rossby et al*., 2010; *Worst et al*., 2014]. XBT (and ADCP) data are available via the Oleander Project website (e.g., http://www.po.gso.uri.edu/rafos/research/ole/index.html). The 37 year record of Oleander XBT transects (1977–2013) has a temporal resolution averaging 14 transects per year. Monthly representation in each year varies, with the fewest transects generally occurring in February and the most in May. Data before 2008 are primarily from the first part of the Bermuda-bound Oleander crossings, with XBTs launched over the MAB shelf, slope, and to approximately the Gulf Stream North Wall with sampling concentrated near the shelfbreak. Starting in 2008, ship riders increased the number of XBTs launched, allowing for sampling to cover the entire span between New Jersey and Bermuda. This is reflected in the

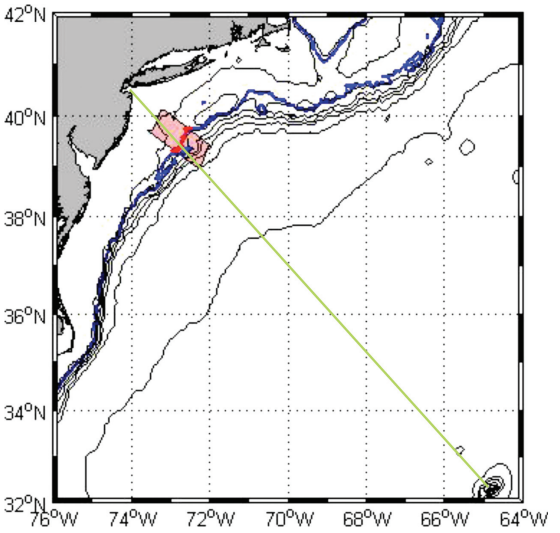

Figure 2. Map of the nominal CMV Oleander route (green line) and the study area (red box) with the 80 m isobath (blue and red contour) used to define $x = 0$ km in the cross-shelf coordinate system. Black contours indicate the 50, 100, 200, 500, 1000, 2000, and 4000 m isobaths.

increase in the average casts per cruise, which is 19 before 2008 and over 33 from 2008 onward. In 2011, an automated XBT launcher replaced the ship rider and continued sampling covering the entire Bermuda-bound route.

The analyses presented below focus on the shelf and upper slope, where data coverage is good over the full 37 year period. The records from 2008 onward report data at 2 m depth interval, while data before 2008 have a varying (and lower) vertical resolution. Compilation of individual CMV Oleander XBT casts to derive a climatology of the MAB cross-shelf temperature structure as well as time series of monthly, seasonally, and annually averaged cross sections is described in section 3.3.

3.2. Sea Level

A time series of the composite coastal sea level since 1970 in the MAB, Gulf of Maine, and Scotian Shelf is generated with data from 12 tide gauge stations between Duck Harbor, North Carolina and North Sydney, Nova Scotia (available from the Permanent Service for Mean Sea Level [*Woodworth and Player*, 2003]) based on the method described in *Andres et al.* [2013]. Briefly, the region's "composite coastal sea level anomaly" is calculated by detrending the annually averaged sea levels from the 12 stations and calculating the means of the residual sea level anomalies across the 12 stations. The "composite trend" is the mean of the 12 stations' trends. The time series of the composite coastal sea level anomaly is well correlated with the anomalies at the individual stations and is an index of the regional-scale interannual coastal sea level variability. A subset of these 12 tide stations were used in the analysis of *Li et al.* [2014], who found that sea level slopes across the Scotian Shelf and Gulf of Maine are correlated with the along-shelf wind stress at interannual scales, consistent with the correlation between coastal sea level and wind stress for the entire 12-station region from North Carolina to Nova Scotia [*Andres et al.*, 2013].

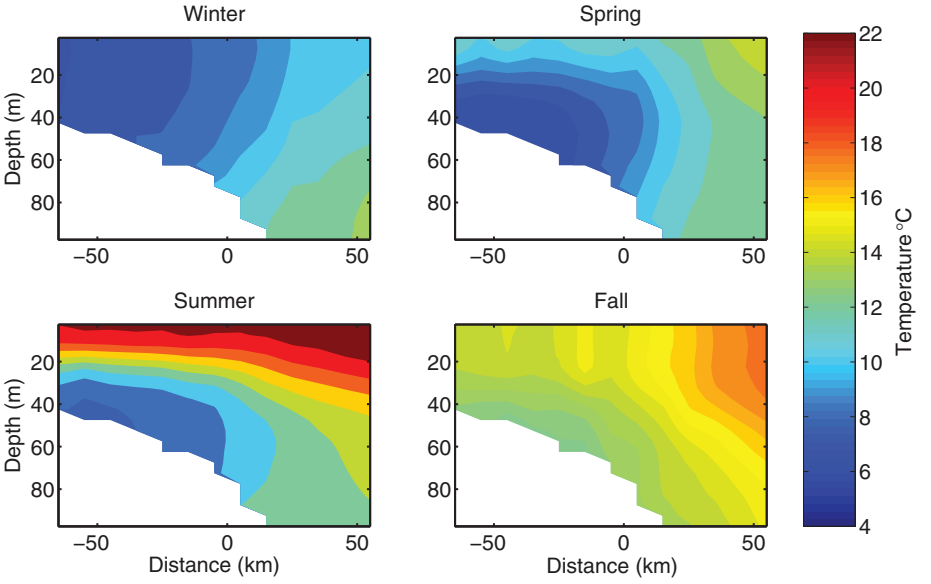

Figure 3. Seasonal climatology of cross-shelf MAB temperature structure produced from the Oleander XBTs.

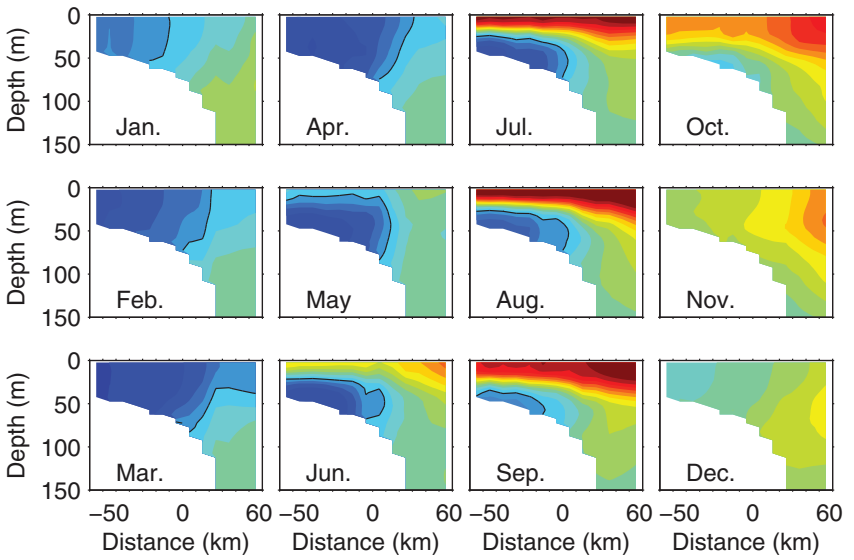

Figure 4. Monthly climatology of cross-shelf MAB temperature sections produced from the Oleander XBTs. Temperature scale as in Figure 3 with the 10°C isotherm contoured (black).

3.3. Generating Average Temperature Sections From Individual XBT Transects

XBT data are downloaded from http://po.msrc.sunysb.edu/Oleander/XBT/NOAA_XBT.html and compiled into a standard format from the two varied formats, which changed in 2008. Once compiled, the temperature data are quality controlled by binning all data (from all months) in 5 m depth bins and eliminating measurements over three standard deviations from each bin's overall mean. Individual casts are then hand analyzed for any patterns in the deeper ocean (defined as below 100 m depth) that could be because of poor data quality. Shallow temperatures are not further corrected as the high variability in the upper water column makes identifying anomalies in the data very difficult. Below this surface layer, XBT-measured temperature generally is found to decrease with increasing depth, as expected. The year 2008 is the only year found to have XBT casts with obvious errors in the subsurface measurements in which anomalous measurements, defined as temperature differences of over 0.5°C between neighboring vertical bins (with bins at a 2 m depth interval), are eliminated and replaced by values interpolated between good points along the temperature profile.

After quality control, temperature data from individual casts are used to generate temperature sections across the MAB shelf and upper slope. Individual CMV Oleander tracks vary somewhat between the crossings and the software developed by Chris Linder [*Linder et al.*, 2006 and available for download at http://www.whoi.edu/science/po/people/clinder/software_climo _xshelf.html] is adopted to bin the quality-controlled temperature measurements within a user-defined area (red box in Figure 2) onto a common cross-shelf grid with 10 km horizontal and 5 m vertical resolution. The cross-shelf position of each cast, x, is defined by the shortest distance between the cast and the 80 m isobath and x increases toward Bermuda. The 80 m isobath is the mean position of the foot of the shelfbreak front off New Jersey [*Linder and Gawarkiewicz*, 1998]. Along the mean path of the CMV Oleander, $x = 0$ km falls near 39.39°N, 72.76°W. The area within which XBT casts are gridded extends from $x = -70$ km (onshore of the 80 m isobath, nominally at the 40 m isobath) to $x = 60$ km (over the upper slope). Though XBT measurements are also available on the inner shelf (onshore of the 40 m isobath), these data are not included in the analysis here since the contorted topography in these shallow waters leads to ambiguity in mapping the individual transects onto a common cross-shelf grid and because this study is focused on processes occurring on the outer shelf and upper slope. In addition, temperature changes in waters shallower than 40 m would likely be strongly affected by the frequency of coastal upwelling, which complicates the analysis as we are primarily focused on the temporal and spatial warming of the Cold Pool water mass.

After binning the data into the cross-shelf grid, monthly averaged temperature cross sections for the shelf and upper slope are produced from the quality-controlled XBT data for each month from 1977 through 2013 for -60 km $\leq x \leq 70$ km (444 total months). Temperature data for those months without sufficient

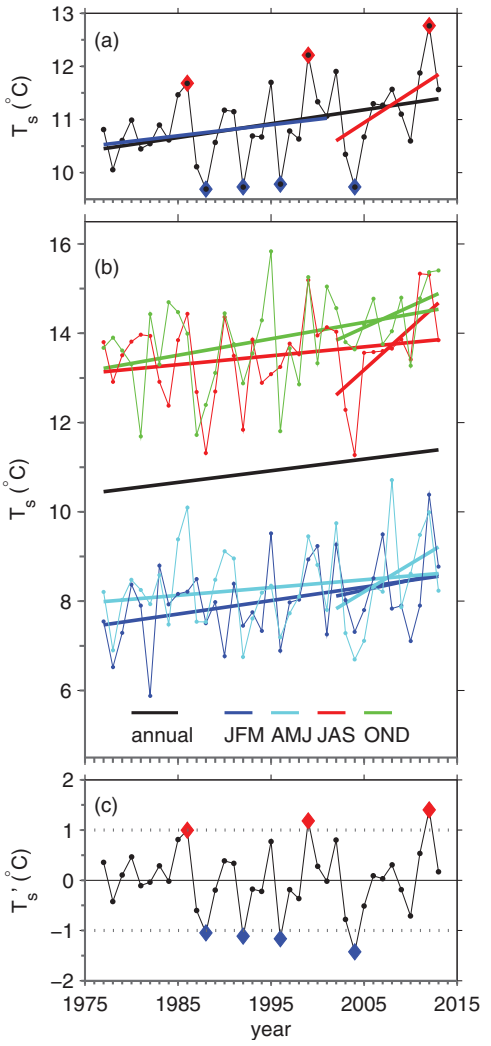

Figure 5. (a) Time series of average shelf temperature represented by T_s (black dots). Linear trends are also shown: the 37 year trend (black line) is 0.026°C yr^{-1}, the 1977–2001 trend (blue line) is 0.021°C yr^{-1}, and the 2002–2013 trend (red line) is 0.11°C yr^{-1} (see Table 1). The three most anomalous warm years (red diamonds) and the four most anomalous cold years (blue diamonds), relative to the 37 year trend, are highlighted. (b) Time series of the seasonal averages of XBT temperatures spatially averaged over the shelf; the 37 year (1977–2013) and the recent (2002–2013) trends are indicated (values are listed in Table 1) and the 37 year T_s trend (black line) as in Figure 2a. (c) T_s' (calculated by removing the 37 year trend from T_s) with the most anomalous warm ($T_s' > 1$°C) and cold ($T_s' < -1$°C) years highlighted (red and blue, respectively).

data over the shelf, defined as months with fewer than 50 individual temperature measurements, are replaced with the climatological 1977–2013 average cross section for the specific month. Overall, 81% of the months have sections that are produced from real data rather than the climatological mean. Even in the winter months, when the XBT data are most sparse, real data are used to generate 75% of the sections. (For a further description of statistics during each phase of quality control, binning and averaging, see Appendix A.) Annually averaged and seasonally averaged temperature cross sections are then produced based on these monthly averaged sections. Seasonal cross sections are made using the calendar months (e.g., winter comprises January, February, and March).

4. MAB Climatology and Shelf Heat Content

4.1. Climatology

The 1977–2013 Oleander XBT climatology is produced from the monthly averaged temperature cross-sections that are further averaged by season (Figure 3). This seasonal climatology is consistent with the key seasonal temperature features found in the previous studies of the MAB [e.g., *Linder and Gawarkiewicz*, 1998; *Linder et al*., 2006]. In winter, shelf temperatures are nearly uniform in the vertical due to both convection and increased vertical mixing from stronger winds [*Zhang et al*., 2011]. Temperature shoreward of the shelfbreak ($x < 0$ km) is generally lower than 10°C. The upper slope is somewhat warmer and the subsurface ($z > 60$ m depth) temperature over the upper slope ($x \approx 50$ km) highlights the presence of the Upper Slope Thermostad (~12–14°C) just offshore of the shelf [*Wright and Parker*, 1976]. In spring, surface heating begins to stratify the water column over the shelf and an isolated pool of subsurface waters colder than 10°C begins to form the "cold pool" [*Houghton et al*., 1982]. This feature persists through the summer season as the cold pool is preserved because of the weak vertical mixing [*Wallace*, 1994] and enhanced stratification because of heat input through solar insolation. In the summer climatology, the surface waters are ~16°C greater than the cold pool temperatures. During fall, frequent storms erase the stratification and mix the deep cold pool waters with the warmer surface layer [*Rasmussen et al*., 2004]. This vertical mixing in fall destroys the seasonal thermocline and leads to vertically uniform temperatures on the shelf, as in winter [*Lentz et al*., 2003]. Interestingly, this fall mixing leads to a summer-to-fall *increase* in near-bottom temperatures on the shelf. In fall, there is also a relatively strong horizontal temperature gradient with cooler waters onshore and warmer waters over the upper slope.

Although the features captured in the Oleander XBT seasonal climatology are not surprising or new, they do provide evidence that the CMV Oleander samples at sufficiently fine temporal and spatial scales to resolve the

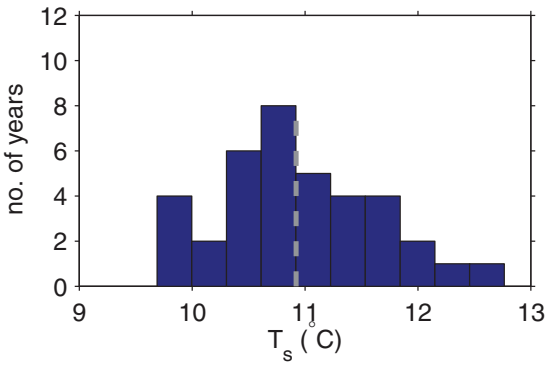

Figure 6. Histogram of T_s with the 37 year mean indicated (dashed line). The interval for the bars is 0.3°C.

seasonal evolution of the vertical and cross-shelf thermal structure. Furthermore, with strong monthly representation throughout the 37 year period spanned by the measurements, even the monthly climatology (Figure 4) represents these known shelf thermal features with fidelity. In the monthly climatology, the cold pool is seen to persist from May through August, with remnants of the cool pool in September and October.

In the following, the time series of monthly averaged sections are first annually averaged. These annually averaged sections are then used to examine the interannual and low-frequency (trends and decadal-scale) variability on the MAB shelf over the 37 year period from 1977 to 2013.

4.2. The Shelf's Time-Varying Heat Content

Since surface temperature variations may be decoupled from subsurface processes, the Oleander temperature sections provide a useful complement to the region's satellite SST record. The Oleander temperature sections are used here to estimate changes in MAB shelf heat content at interannual and longer timescales. Each annually averaged temperature section is spatially averaged over $-60\ \text{km} \le x \le 0\ \text{km}$ (i.e., shoreward of the 80 m isobath) to generate an annual average shelf temperature, T_s, for each year from 1970 to 2013 (Figure 5). This area purposely excludes the upper slope, where the salient dynamics are likely somewhat independent of those on the shelf (as corroborated by the differences in stratification on the shelf and upper slope in the seasonal and monthly climatologies in Figures 3 and 4).

The mean T_s is 10.9°C and the range over the 37 year record is 3°C (Figure 6). The shelf's largest average temperature ($T_s = 12.8$°C) occurs in 2012 (Figure 7, top), consistent with the previous reports that 2012 stands out as an anomalously warm year from the Gulf of Maine to Cape Hatteras [*Mills et al*., 2013; *Chen et al*., 2014]. The shelf's ocean heat content during this warm year, relative to the mean heat content (i.e., with $\bar{T} = 10.9$°C), can be estimated:

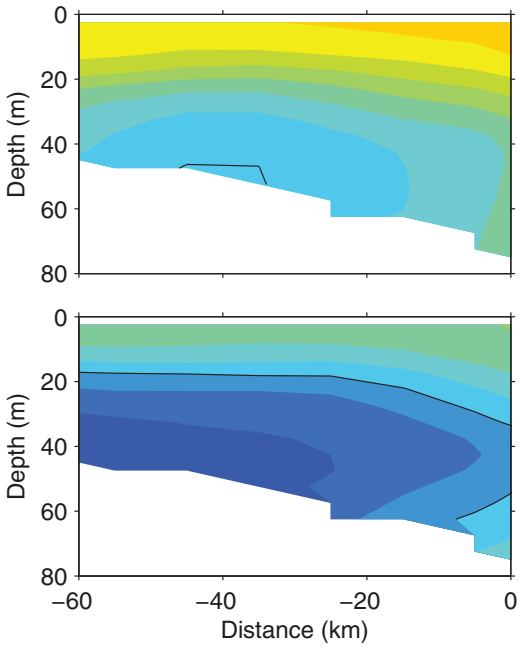

Figure 7. Annually averaged temperature sections for the years with (top) highest (2012) and (bottom) lowest (2008) overall shelf temperature (T_s). Color bar is as in Figure 3 with contours at 1°C interval and the 10°C isotherm is highlighted (black).

$$\Delta OHC = \rho_o A C_p (T_s - \bar{T}_s). \quad (2)$$

Here ΔOHC is the shelf's heat content change per unit length in the along-shelf direction, ρ_o is water density on the shelf (~1025 kg m^{-3}), A is the cross-shelf area at the Oleander line (~3.6×10^6 m^2), and C_p is the specific heat of seawater (3850 J kg^{-1} °C^{-1}). For $T_s = 12.8$°C, ΔOHC is 2.7×10^{10} kJ m^{-1} (i.e., 17% increase in heat content relative to the mean). The year with the coldest average temperature ($T_s = 9.7$°C) is 1988 (Figure 7, bottom) and during this year ΔOHC is -1.7×10^{10} kJ m^{-1} (11% decrease in heat content relative to the mean).

5. MAB Temperature Variability

Although shelf heat content (which is proportional to T_s) exhibits both interannual variability and long-term trend (each discussed further below), it is noteworthy that the years with lowest heat content (blue diamonds in Figure 5) have relatively uniform T_s over the

Table 1. Annual and Seasonal Temperature Trends (°C yr^{-1})

	1977–2013[a]	2002–2013[a]	2004–2012[a]
Annual	0.026 ± 0.001	0.11 ± 0.02	0.24 ± 0.03
Winter	0.030	0.045	0.136
Spring	0.018	0.126	0.342
Summer	0.020	0.188	0.357
Fall	0.037	0.095	0.112
	1875–2007[b]	1982–2012[c]	2004–2012[c]
MAB	0.007 ± 0.003		
Gulf of Maine	0.010 ± 0.003	0.026	0.26

[a]This study. Error bounds indicate the confidence intervals at the 95% level using a Student's *t* test with each T_s' treated as independent.
[b]*Shearman and Lentz* [2010].
[c]*Mills et al*. [2013].

37 year record with T_s that is consistently 1.1–1.2°C below the mean during the four coldest years (1999, 1992, 1996, and 2004). In contrast, the years with highest heat content (red diamonds in Figure 5) exhibit progressively increasing T_s (0.8, 1.3, and 1.9°C above the mean in 1986, 1999, and 2012, respectively).

5.1. Temperature Trend

As noted above, T_s (calculated from the annually averaged temperature sections, spatially averaged over the shelf shoreward of the 80 m isobath at $x = 0$ km) has been trending upward since 1977 (Figure 5a, black line). The rate of increase over 37 years is 0.026°C yr^{-1} ± 0.001 (Table 1), which is about four times greater than the centennial trend (1875–2007) reported by *Shearman and Lentz* [2010] for near-surface temperatures in the MAB. (Here as in *Shearman and Lentz* [2010], the confidence intervals for the trends are calculated using a Student's *t* test with each annual mean treated as an independent measure and are reported at the 95% confidence level.) More recently, the T_s trend has accelerated further; the 2002–2013 trend is 0.11°C°yr^{-1} ± 0.02 (Figure 5a, red line). This recent trend is five times larger than the pre-2002 trend (0.022 °C yr^{-1}) and an order of magnitude larger than the 1875–2007 trend.

The 37 year warming trend on the shelf identified with the XBT data is not confined to a single season (Figure 5b). Concurrently with the increasing T_s (which represents the annual averages), the shelf temperatures averaged within each season are also increasing. The 37 year trends are more pronounced in fall/winter than in spring/summer (Table 1). In contrast to these 37 year seasonal trends, the recent (2002–2013) amplified T_s trend is accompanied by shelf temperature increases that are most pronounced during summer. This suggestion of the recent amplification of the T_s trend driven by warming of MAB summers is consistent with the results – based on the sea surface temperatures from the International Comprehensive Ocean Atmosphere Data Set (ICODS) – that the annual range of SSTs experienced on the shelf has been increasing with winter SSTs which remain fairly steady as summer SSTs increase [*Friedland and Hare*, 2007].

Both the long-term (37 years) T_s trend at the Oleander line and the recent acceleration in warming there are consistent with a previous study based on SSTs (produced by the Group for High-Resolution Sea Surface Temperature, GHRSST) in the Gulf of Maine, which finds an accelerated rate of temperature increase there since 2004 [*Mills et al*., 2013]. This suggests that the processes associated with the accelerated warming are not isolated, but are widespread over the shelves of the northwestern North Atlantic. It is important to note, however, that 2004 and 2012 were extreme cold and warm years, respectively (see Figure 5c and section 5.2). The 2004–2012 trend reported for the Gulf of Maine GHRSST data is similar to the trend found in the MAB based on the Oleander XBT records for the identical time period (0.24°C yr^{-1}). However, shifting the endpoints of the MAB trend calculation to less extreme years (2002–2013) reduces the T_s trend by a factor of two (Table 1).

Despite this ambiguity in quantifying the trends in short time series that have strong interannual variability, the Oleander XBT data do clearly show that shelf warming is not confined to a thin SST boundary near the surface (observed with satellites), but occurs throughout the water column (observed with the XBTs). This warming at depth is demonstrated by a cross-shelf section showing the temperature trends within each bin of the annually averaged mapped temperatures (Figure 8, top). There is a positive trend in each bin on the shelf and the warming trends are strongest at the surface and near the bottom, with a minimum midwater column. Also, over the 37 year record there is weak warming over the upper slope (note that the temperatures offshore of the 80-m isobath, although indicated in the plots, do not contribute to the T_s calculations).

This cross-section map of the 37 year trends is further decomposed into the trends from 1977 to 2001 and from 2002 to 2013. The warming trends pre-2002 (Figure 8, middle) are modest and there is little warming over the upper slope. The warming is most pronounced at the bottom, just onshore of the 80 m isobath. This is near the mean position of the foot of the shelfbreak jet [*Linder and Gawarkiewicz*, 1998] and suggests

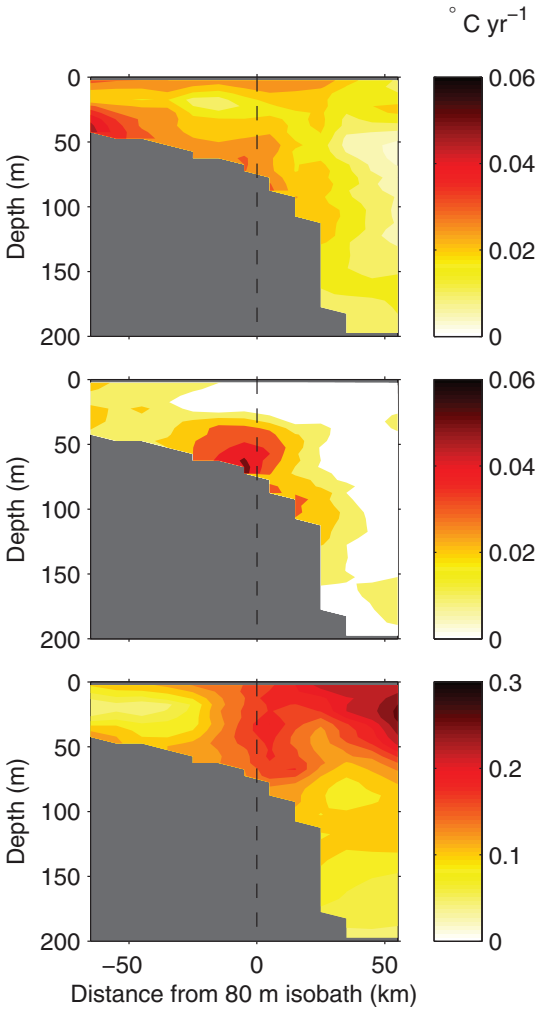

Figure 8. Trends of the annually averaged temperatures in each bin along the Oleander line for (top) 1977–2013, (middle) 1977–2001, and (bottom) 2002–2013. Dashed line indicates the 80 m isobath (T_s comprises contributions from temperatures shoreward of this). Scale in the bottom plot is five times greater than that in the other plots.

that processes associated with cross-shelf translation of the shelfbreak front may play a role in the long-term heating on the shelf.

The trends that contribute to the recent accelerated warming exhibit a very different pattern (Figure 8, bottom). (Note that the scale here is five times as large as that in the top and middle plots.) Over 2002–2013, there is strong warming on the offshore edge of the shelf from the surface to the bottom. There is also accelerated warming on the upper slope. Though the upper slope does not contribute directly to the calculated T_s trend (which is area averaged over only the shelf), the pattern does indicate that the shelf warming may be driven by shelf/slope interactions. It is possible that 2002–2013 experienced the arrival of more subtropical waters to the Slope Sea via more frequent or more intense warm core rings [*Ramp et al*., 1983; *Joyce et al*., 1992; *Gawarkiewicz et al*., 2001] or diverted Gulf Stream paths [*Gawarkiewicz et al*., 2012]. Alternatively, the warming trend in the Slope Sea near the Oleander line could be related to the waters advected from the north [*Peña-Molino and Joyce*, 2008].

5.2. Interannual Temperature Variability at the Oleander Line

In addition to the trends discussed above, T_s exhibits significant year-to-year variability throughout the 37 year record. To examine the interannual changes in the temperature structure along the Oleander line, T_s is first detrended (removing the entire 37 year trend) to produce a time series of interannual shelf temperature anomalies, T_s' (Figure 5c). Years with $|T_s'| > 1°C$ are identified as the most anomalous years. The annually averaged temperature sections for the 3 years with maximum T_s' (1986, 1999, and 2012, red diamonds in Figure 5) are averaged together. From this warm average, the 37 year mean temperature section is subtracted to give a composite section of warm-year temperature anomalies (Figure 9, top). Likewise, the annually averaged temperature sections for the 4 years with minimum T_s' (1988, 1992, 1996, and 2004, blue diamonds in Figure 5) are averaged together and the 37 year mean temperature section is subtracted to build a composite section of cold-year anomalies (Figure 9, bottom). The warm-year and cold-year anomaly sections each have the strongest magnitude temperature anomalies near the shelfbreak. The warm-year composite's peak anomaly is found between 0 and 15 km offshore of the 80 m isobath while the cold year composite's peak anomaly is directly over the 80 m isobath. This indicates that – as with the low-frequency variations associated with the long-term trends—the interannual variations in T_s on the shelf are most sensitive to processes occurring near the shelfbreak. Interestingly, the anomalies in the warm composite and the cold composite sections are not strongest near the surface, suggesting that interannual changes in the local atmospheric heat flux are not the dominant process affecting interannual temperature variability on the shelf (T_s'). However, a careful analysis of the 2012 warm anomaly has indicated that the MAB SSTs (as well as the subsurface shelf temperatures) in 2012 were controlled by anomalous atmospheric heat flux [*Chen et al*., 2014]. These conflicting results suggest that multiple processes strongly influence shelf temperatures with local heat flux

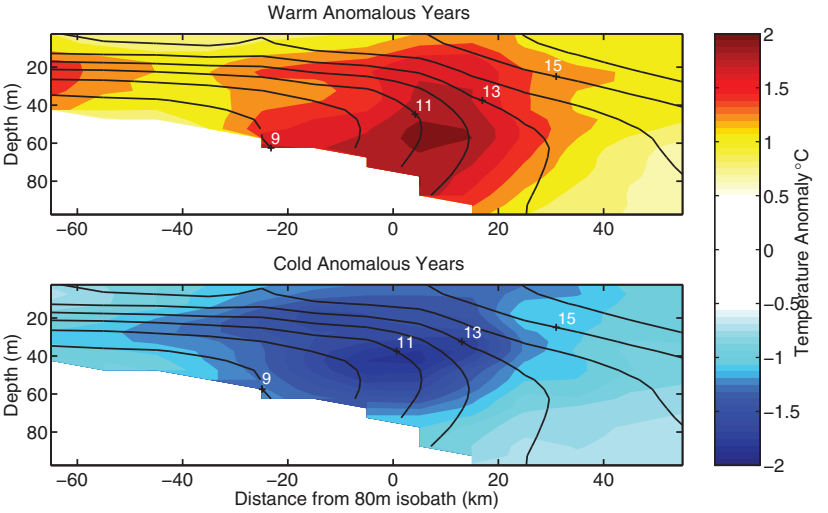

Figure 9. Sections of temperature anomalies for the warm-year composite (top) generated from annually averaged temperature sections for 1986, 1999 and 2012, and the cold-year composite (bottom) generated from the annually averaged temperature sections for 1988, 1992, 1996, and 2004. For reference, black contours and white labels (°C) indicate the mean temperature section.

[e.g., *Chen et al*., 2014], cross-shelf exchange between the shelf and Slope Sea (this work), and along-shelf advection [e.g., *Shearman and Lentz*, 2010], each playing a significant role in setting the shelf's heat budget.

5.3. Temperature and Sea Level

As the global ocean warms [*Abraham et al*., 2013], thermal expansion leads to an increase in the global mean sea level [*Stammer et al*., 2013] and mean sea level on the shelves rises simply because the rest of the ocean is expanding (the thermal expansion on the shelves leads to a negligible contribution to the ocean's overall volume increase). However, since coastal sea level between Cape Hatteras and Nova Scotia is increasing at a rate higher than the global mean rate [e.g., *Sallenger et al*., 2012] and since both T_s and sea level records exhibit recently accelerated rates of increase here, it is tempting to assume that the trends in T_s (Figure 5) and in the composite coastal sea level (Figure 10) are linked by a local (shelf) thermosteric effect, however this is not the case. Using (equation (1)), the rates of warming observed with the Oleander XBTs for various time periods (i.e., the T_s trends) can be used to estimate the portion of sea level rise caused by local warming (Table 2). This comparison shows that the sea level increases that can be accounted for by the T_s trends are an order of magnitude too small to account for the observed rate of sea level rise between Cape Hatteras and Nova Scotia that is in excess of the global mean rate (compare 4th and 6th columns Table 2). Hence, to first order, the increased sea levels here cannot be explained by the thermal expansion associated with the warming shelf and the "hotspot of sea level rise" identified by *Sallenger et al*. [2012] is not a local (shelf) thermosteric effect. However, in this region, salinity variations are a critical factor in setting the density variations observed on the shelf [e.g., *Mountain* 2003 and references therein]; the Oleander XBT data cannot address whether the accelerated increase in sea level along the coast is a local halosteric effect. Finally, there is evidence that in some locations regional (i.e., in the nearby open ocean) steric sea level changes are communicated across a sloping bottom to the shelf and coast [*Bingham and Hughes*, 2012], though it is not yet clear whether this could be the case for the Slope Sea and the neighboring MAB shelf (since there is an intervening current, the Shelfbreak jet).

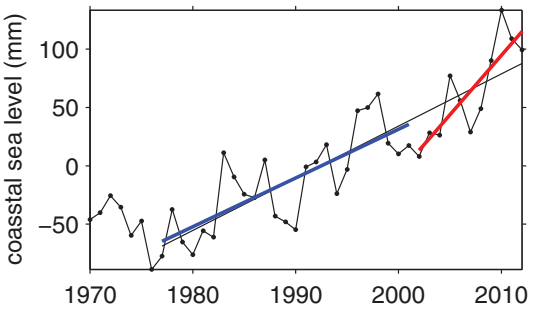

Figure 10. Total composite coastal sea level calculated from the annually averaged tide records from 12 stations between Duck, North Carolina and North Sydney, Nova Scotia. Adapted from *Andres et al*. [2013]. Lines indicate the trends for 1977–2012 (black), 1977–2001 (blue), and 2002–2012 (red) with the slopes listed in Table 1 (column 5).

Examination of the interannual variability shows, as with the trends discussed above, the interannual variability in coastal sea level is not a thermosteric effect. If it were, shelf

Table 2. Sea Level Rise Attributed to Shelf Warming Compared With the Observed Excess Sea Level Rise on the Shelf

Number of Years	Range	Shelf Warming[a] (°C yr^{-1})	Rise Due to Warming[b] (mm yr^{-1})	Observed Rise[c] (mm yr^{-1})	Excess Rise[d] (mm yr^{-1})
36	1977–2012	0.025	0.18	4.5	1.2
25	1977–2001	0.021	0.15	4.2	1
11	2002–2012	0.129	0.90	10.2	7

[a]Calculated from T_s linear trends (Figure 5).
[b]Calculated from the shelf warming rate and equation (1) with an average shelf depth $D = 40$ m, and $\alpha = 1.75 \times 10^{-4}$ (for seawater at 10.9°C, salinity = 34.5, and pressure = 20 dbar).
[c]Calculated from the linear trends in composite coastal sea level [*Andres et al.*, 2013] and Figure 10.
[d]Difference between the global mean sea level rise rate for 1993–2009 (3.2 mm yr^{-1}) [*Church and White*, 2011] and the rate of rise observed on the shelf. Using the reported trend for 1961–2009 (1.9 mm yr^{-1}), leads to an even greater mismatch between the excess rise and the rise calculated from the warming.

temperature anomalies would be positively correlated with the concurrent coastal sea level anomalies. However, at zero lag, T_s' is not significantly correlated with composite coastal sea level anomalies (Figure 11, top) and the calculated correlation is negative (though insignificant).

However, when a 2 year lag is introduced to T_s' (Figure 12), there is a striking and statistically significant positive correlation with sea level anomalies. The 2 year lagged correlation, r, calculated with a 37 year trend removed from each record (i.e., over 1975–2011 for sea level and 1977–2013 for temperature) is 0.59. Accounting for the autocorrelation of T_s' and of sea level anomaly (Figure 11, bottom)—which indicate an integral time scale of about 1.5 years for each record and hence 12 effective degrees of freedom—this correlation is significant above the 95% confidence level.

This significant correlation suggests that when coastal sea level peaks, shelf waters experience an anomalous warming 2 years later. The mechanism underlying this correlation is being explored elsewhere and may be related to changes in along-shelf advection associated with interannual variability in the regional wind stress. The interannual changes in along-shore wind stress have been shown to correlate with interannual variability in cross-shelf sea surface slope and presumably (via geostrophy) the along-shelf transport [*Andres et al.*, 2013; *Li et al.*, 2014]. Here we simply note that about one-third of the variance in T_s' is explained by composite coastal sea level anomalies from 2 years earlier.

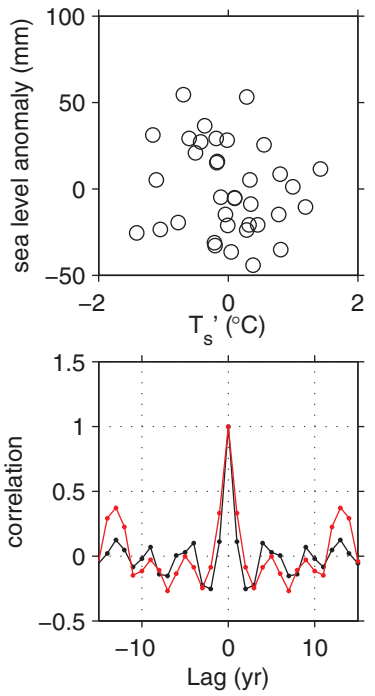

Figure 11. (top) Comparison of the annually averaged shelf temperature anomalies (T'_s) and the concurrent composite coastal sea level anomalies, each detrended from 1977 to 2012. (bottom) Autocorrelations for sea level anomalies (red) and for T'_s (black).

We also note that 2 year lags in the northwest Atlantic shelf system are conspicuous: similar lags have been reported between climate indices and various indices on the shelf [*Hare and Kane*, 2012 and references therein]. Furthermore, *Hare and Kane* [2012] report a changing link with the North Atlantic Oscillation (NAO), a climate index related to long-term atmospheric variability representing the sea level pressure difference between the Azores and Greenland [*Hurrell*, 1995]). Two year lagged correlations of NAO are statistically significant over some periods but not over others with (1) local shelf environmental variables (e.g., temperature) and (2) with biological variables related to zooplankton. The Oleander XBT data reported here also suggest a changing relationship between NAO and the shelf system in the northwestern North Atlantic. Over the full 1977–2013 period, T_s and winter NAO index are not significantly correlated (with both records linearly detrended); but over the most recent 20 years (1993–2013), the correlation between NAO and T_s is positive and significant at the 95% confidence level (correlation coefficient, $r = 0.43$, with both records detrended).

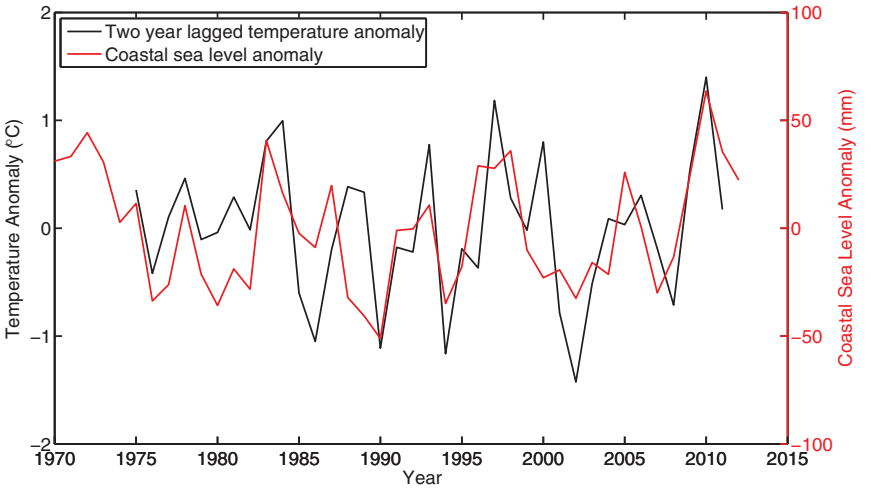

Figure 12. Coastal composite sea level anomalies (red) and the 2 year lagged temperature anomalies (T'_s, black).

Investigations into the relationships between the Oleander XBT sections and other shelf indices and into the shelf's regional responses to basin-wide climate variability (as represented by the NAO index) are ongoing.

6. Conclusions

The CMV Oleander XBT data set spans almost 4 decades and provides an invaluable resource for identifying interannual to decadal variability on the MAB shelf. Since the spatial and temporal scales of the Oleander XBT data set resolve some of the critical shelf processes (such as the generation and erosion of the cold pool), one can use the data set not only to identify change, but also to explore the mechanisms causing the change. The fidelity of the seasonal and monthly climatologies generated from the Oleander monthly mean temperature sections to previous climatologies demonstrates the utility of this data set as a means to monitor and predict change.

With the Oleander data, the recent accelerated temperature trend found in the Gulf of Maine [*Mills et al.* 2013] has now been also identified in the MAB not only as a surface feature, but as a full-water column signal. The

Table 3. Summary Statistics for XBT Data Quality Control Steps

	Preliminary Data	First Quality Control	Initial Software	Binned Data on Shelf	Binned Data Off Shelf
Cruises	516	516			
Monthly representation			372	361	361
Casts	10,293	~10,200	3,688	~2000	~1600
Data points	822,209	820,079	83,842		
Cruises per year	14	14			
Real months per year			10.05	9.76	9.76
Casts per cruise	19.94	~19.7	n/a	n/a	n/a
Casts per month			8.3	~4.5	~3.6
Casts per real month			9.91	~5.5	~4.4
January	42	42	31	29	29
February	31	31	26	24	24
March	42	42	33	30	30
April	39	39	28	26	26
May	53	53	35	35	35
June	44	44	34	33	33
July	48	48	33	32	32
August	42	42	32	29	29
September	39	39	30	30	30
October	48	48	32	30	30
November	45	45	32	30	30
December	43	43	34	33	33

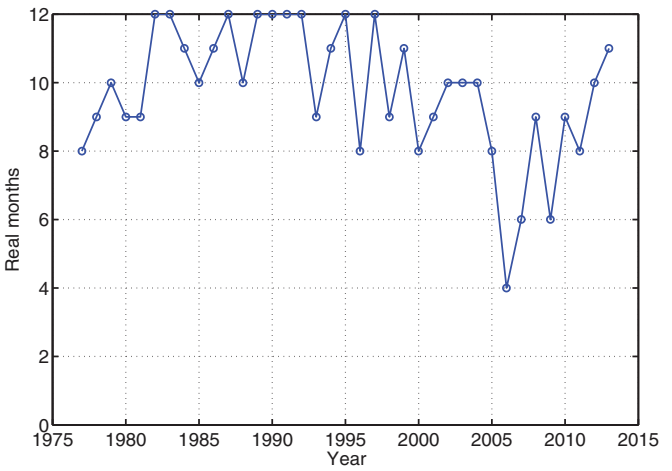

Figure 13. The number of monthly averaged temperature cross sections in each year that are generated from that year's Oleander XBT data. The remaining months' sections in a given year are replaced (due to insufficient XBT data coverage in a given month) with the monthly climatology calculated from the balance of the 37 year XBT record.

MAB shelf warming, although dramatic, is too small to account either for the higher rate of sea level rise relative to the global mean rate or for the recent acceleration in rates between Cape Hatteras and Nova Scotia. One would need the same temperature increase over hundreds of meters, rather than tens of meters, to account for the shelf's excess (relative to the global mean) sea level trend.

The Oleander data set highlights the importance of processes occurring along the shelfbreak both in controlling the shelf's long-term (37 years) temperature trends and the interannual temperature variability. In contrast, the recent acceleration in the temperature trends seems to be related to the Slope Sea and shelf/open-ocean interactions. Finally, the striking 2 year lagged correlations between annually averaged coastal sea level anomaly and T_s' suggest that tide gauge measurements from the MAB, Gulf of Maine, and Scotian Shelf present a potentially useful (and readily accessible) predictor for interannual variations in the temperature conditions on the shelves.

Variability on the shelves between Cape Hatteras and Nova Scotia has important societal impacts. Strong interannual variability in sea levels complicates the identification of accelerated trends in the northwestern North Atlantic and uncertainty in predictions of future change can lead to contentious management decisions [*Phillips*, 2012]. Furthermore, commercially important fish species may be sensitive to changes in shelf temperature and circulation [*Nye et al.*, 2009]. Hence, shelf temperature anomalies have the potential to negatively impact local fish populations and the related economies. As we are becoming increasingly dependent on the predictions from models to make policy decisions, continued in situ ocean observations serve as a critical tool, both as a means to validate the models and to explore the dynamical underpinnings of observed variability.

Appendix A

The summary statistics for various phases of the Oleander XBT data processing (described in section 3.1) are shown in Table 3. "Preliminary data" refer to the data downloaded directly from the website. "First quality control" refers to the data after removing 2008 oddities and measurements over 3 standard deviations from the mean temperature in each 5 m vertical bin. "Initial software" is after running the Linder [*Linder et al.*, 2006] software with a minimum threshold of 50 measurements in a given month to generate the monthly average (below this threshold, the monthly climatological value is used, see also Figure 13). The last two columns in Table 3 refer to the data which have been hand corrected from the initial software run to eliminate months without enough spatial resolution in the onshore bins and in the offshore bins.

Acknowledgments

The XBT data along the Oleander line were collected through NOAA's Northeast Fisheries Science Center (NOAA/NEFSC) Ship of Opportunity Program (SOOP), with data collection presently continuing under the NSF-funded Oleander Program. These data can be accessed at http://po.msrc.sunysb.edu/Oleander/XBT/NOAA_XBT.html. The software used to map the XBT data is available at http://www.whoi.edu/science/po/people/clinder/software_climo _xshelf.html. Sea level data are available through the Permanent Service for Mean Sea Level and can be accessed at http://www.psmsl.org. J.F. was supported as a Woods Hole Oceanographic Institution Summer Student Fellow by the National Science Foundation's Research Experiences for Undergraduates through OCE-0649139. M.A. received support through OCE-1332667 and G.G. through OCE-1435602. We gratefully acknowledge Robert Benway (NOAA) for his many years of support of Oleander data collection via NOAA's Voluntary Observing Ship Program. We extend additional thanks to the Neptune Group Ltd. Bermuda Container Line and to the captain and crew of the CMV Oleander for their long-term commitment to data collection and to Kathy Donohue (URI) and Tom Rossby (URI) and Charlie Flagg (SUNY Stony Brook) and to Chris Linder (WHOI) for help with the mapping. This work benefited from helpful comments provided by Jon Hare and an anonymous reviewer.

References

Abraham, J. P., et al. (2013), A review of global ocean temperature observations: Implications for ocean heat content estimates and climate change, *Rev. Geophys.*, *51*, 450–483, doi:10.1002/rog.20022.

Andres, M., G. G. Gawarkiewicz, and J. M. Toole (2013), Interannual sea level variability in the western North Atlantic: Regional forcing and remote response, *Geophys. Res. Lett.*, *40*, 5915–5919, doi:10.1002/2013GL058013.

Atkinson, L., J. Blanton, W. Chandler, and T. Lee (1983), Climatology of the southeastern United States continental shelf waters, *J. Geophys. Res.*, *88*, 4705–4718.

Chen, K., G. G. Gawarkiewicz, S. J. Lentz, and J. M. Bane (2014), Diagnosing the warming of the Northeastern U.S. Coastal Ocean in 2012: A linkage between the atmospheric jet stream variability and ocean response, *J. Geophys. Res. Oceans*, *119*, 218–227, doi:10.1002/2013JC009393.

Church, J. A., and N. J. White (2011), Sea-level rise from the late 19th to the early 21st century, *Surv. Geophys.*, *32*, 585–602, doi:10.1007/s10712-011-9119-1.
Churchill, J. H., and G. G. Gawarkiewicz (2012), Pathways of shelf water export from the Hatteras shelf and slope, *J. Geophys. Res.*, *117*, C08023, doi:10.1029/2012JC007995.
Csanady, G. T., and P. Hamilton (1988), Circulation of slopewater, *Cont. Shelf Res.*, *8*(5–7), 565–624.
Ford, W., J. Longard, and R. Banks (1952), On the nature, occurrence, and origin of cold, low salinity water along the edge of the Gulf Stream, *J. Mar. Res.*, *11*, 281–293.
Ezer, T., L. P. Atkinson, W. B. Corlett, and J. L. Blanco (2013), Gulf Stream's induced sea level rise and variability along the U.S. mid-Atlantic coast, *J. Geophys. Res. Oceans*, *118*, 1–13, doi:10.1002/jgrc.20091.
Flagg, C., G. Schwartze, E. Gottlieb, and T. Rossby (1998), Operating an acoustic Doppler current profiler (ADCP) aboard a container vessel, *J. Atmos. Oceanic Technol.*, *15*, 257–271.
Flagg, C. N., M. Dunn, D.-P. Wang, H. T. Rossby, and R. L. Benway (2006), A study of the currents of the outer shelf and upper slope from a decade of shipboard ADCP observations in the Middle Atlantic Bight, *J. Geophys. Res.*, *111*, C06003, doi:10.1029/2005JC003116.
Frank, K. T., B. Petrie, J. S. Choi, and W. C. Leggett (2005), Trophic cascades in a formerly Cod-dominated ecosystem, *Science*, *308*, 1621, doi:10.1126/science.1113075.
Fratantoni, P. S., and R. S. Pickart (2007), The western North Atlantic shelfbreak current system in summer, *J. Phys. Oceangr.*, *37*, 2509–2533, doi:10.1175/JPO3123.1.
Friedland, K. D., and J. A. Hare (2007), Long-term trends and regime shifts in sea surface temperature on the continental shelf of the northeast United States, *Cont. Shelf Res.*, *27*(18), 2313–2328, doi:10.1016/j.csr.2007.06.001.
Joyce, T. M., J. Dunworth-Baker, R. S. Pickart, D. Torres, and S. Waterman (2005), On the deep western boundary current south of Cape Cod, *Deep Sea Res., Part II*, *52*, 615–625.
Joyce, T. M., J. K. B. Bishop, and O. B. Brown, O. B. (1992), Observations of offshore shelf-water transport induced by a warm-core ring, *Deep Sea Res., Part A*, *39*, S97–S113.
Gawarkiewicz, G. G., and C. Linder (2006), Lagrangian flow patterns north of Cape Hatteras using near-surface drifters, *Prog. Oceanogr.*, *70*, 181–195.
Gawarkiewicz, G. G., F. Bahr, R. C. Beardsley, and K. H. Brink (2001), Interaction of a slope eddy with the shelfbreak front in the Middle Atlantic Bight, *J. Phys. Oceanogr.*, *31*, 2783–2796.
Gawarkiewicz, G. G., J. Churchill, F. Bahr, C. Linder, and C. Marquette (2008), Shelfbreak frontal structure and processes north of Cape Hatteras in winter, *J. Mar. Res.*, *66*, 775–799.
Gawarkiewicz, G. G., R. E. Todd, A. J. Plueddemann, M. Andres, and J. P. Manning (2012), Direct interaction between the Gulf Stream and the shelfbreak south of New England, *Sci. Rep.*, *2*, 553, doi:10.1038/srep00553.
Hare, J. A., and J. Kane (2012), Zooplankton of the Gulf of Maine—A changing perspective, in *American Fisheries Socirty Symposium on Advancing an Ecosystem Approach in the Gulf of Maine*, vol. 79, edited by R. Stephenson et al., pp. 115–137.
Houghton, R., R. Schlitz, R. Beardsley, B. Butman, and J. Chamberlain (1982), The Middle Atlantic Bight cold pool: Evolution of the temperature structure during summer 1979, *J. Phys. Oceanogr.*, *12*, 1019–1029.
Hurrell, J. W. (1995), Decadal trends in the North Atlantic Oscillation: Regional temperatures and precipitation, *Science*, *269*(5224), 676–679.
Lentz, S. J., R. K. Shearman, S. Anderson, A. J. Plueddemann, and J. Edson (2003), Evolution of stratification over the New England shelf during the Coastal Mixing and Optics study, August 1996– June 1997, *J. Geophys. Res.*, *108*(C1), 3008, doi:10.1029/2001JC001121.
Lentz, S. J. (2008), Observations and a model of the mean circulation over the Middle Atlantic Bight continental shelf, *J. Phys. Oceanogr.*, *38*, 1203–1221, doi:10.1175/2007JPO3768.1.
Li, Y., R. Ji, P. S. Fratantoni, C. Chen, J. A. Hare, C. S. Davis, and R. C. Beardsley (2014), Wind-induced interannual variability of sea level slope, alongshelf flow, and surface salinity on the Northwest Atlantic shelf, *J. Geophys. Res. Oceans*, *119*, 2462–2479, doi:10.1002/2013JC009385.
Linder, C. A., and G. G. Gawarkiewicz (1998), A climatology of the shelfbreak front in the Middle Atlantic Bight, *J. Geophys. Res.*, *103*, 18,405–18,423.
Linder, C. A., G.G. Gawarkiewicz, and M. Taylor (2006), Climatological estimation of environmental uncertainty over the Middle Atlantic Bight shelf and slope, *IEEE J. Oceanic Eng.*, *31*(2), 308–324.
Merrifield, M. A., S. T. Merrifield, and G. T. Mitchum (2009), An anomalous recent acceleration of global sea level rise, *J. Clim.*, *22*, 5772–5781, doi:10.1175/2009JCLI2985.1.
Mills, K. E., et al. (2013), Fisheries management in a changing climate: Lessons from the 2012 ocean heat wave in the Northwest Atlantic, *Oceanography*, *26*(2), doi:10.5670/oceanog.2013.27.
Mountain, D. G., (2003), Variability in the properties of Shelf Water in the Middle Atlantic Bight, 1977–1999, *J. Geophys. Res.*, *108*(C1), 3014, doi:10.1029/2001JC001044.
Peña-Molino, B., and T. M. Joyce (2008), Variability in the Slope Water and its relation to the Gulf Stream path, *Geophys. Res. Lett.*, *35*, L03606, doi:10.1029/2007GL032183.
Phillips, L. (2012), US northeast coast is hotspot for rising sea levels, *Nature News*, doi:10.1038/nature. 2012.10880.
Pickart R. S., and D. R. Watts (1990), Deep Western Boundary current variability at Cape Hatteras, *J. Mar. Res.*, *48*, 765–791.
Ramp, S. R., R. C. Beardsley, and R. Legeckis, R (1983), An observation of frontal wave development on a shelf-slope/warm core ring front near the shelf break south of New England, *J. Phys. Oceanogr.*, *13*, 907–912.
Rasmussen, L., G. Gawarkiewicz, W. Owens, and M. Lozier (2005), Slope water, Gulf Stream, and seasonal influences on southern Mid-Atlantic Bight circulation during the fall-winter transition, *J. Geophys. Res.*, *110*, C02009, doi:10.1029/2004JC002311.
Rossby, T., C. Flagg, and K. Donohue (2010), On the variability of Gulf Stream transport from seasonal to decadal timescales, *J. Mar. Res.*, *68*, 503–522.
Rossby, T., C. N. Flagg, K. Donohue, A. Sanchez-Franks, and J. Lillibridge (2014), On the long-term stability of Gulf Stream transport based on 20 years of direct measurements, *Geophys. Res. Lett.*, *41*, 114–120, doi:10.1002/2013GL058636.
Sallenger, A. H., K. S. Doran, and P. A. Howd (2012), Hotspot of accelerated sea-level rise on the Atlantic coast of North America, *Nat. Clim. Change*, *2*, 884–888, doi:10.1038/NClimate1597.
Savidge, D. K., and Bane, J. M. (2001), Wind and Gulf Stream influences on along-shelf transport and off-shelf export at Cape Hatteras, North Carolina, *J. Geophys. Res.*, *106*, 11,505–11,527, doi:10.1029/2000JC000574.
Shearman, R. K., and S. J. Lentz (2010), Long-term sea surface temperature variability along the US East Coast. *J. Phys. Oceanogr.*, *40*, 1004–1017, doi:10.1175/2009JPO4300.1.
Stammer, D., A. Cazenave, R. M. Ponte, and M. E. Tamisiea (2013), Causes for contemporary regional sea level changes, *Ann. Rev. Mar. Sci.*, *5*, 21–46, doi:10.1146/annurev-marine-121211–172406.

Toole, J. M., R. G. Curry, T. M. Joyce, M. McCartney, and B. Peña-Molino (2011), Transport of the North Atlantic Deep Western Boundary Current about 35°N, 70°W: 2004–2008, *Deep Sea Res., Part II*, *58*, 1768–1780.

Wallace, D. W. R. (1994), Anthropogenic chlorofluoromethanes and seasonal mixing rates in the Middle Atlantic Bight, *Deep Sea Res., Part II*, *41*(2-3), 307–324, doi:10.1016/0967-0645(94)90025-6.

Worst, J. S., K.A. Donohue, and T. Rossby (2014), A comparison of vessel-mounted acoustic Doppler current profiler and satellite altimeter estimates of sea surface height and transports between New Jersey and Bermuda along the CMV Oleander route, *J. Atmos. Oceanic Technol.*, *31*, 1422–1433, doi:10.1175/JTECH-D-13–00122.1.

Woodworth, P. L., and R. Player (2003), The permanent service for mean sea level: an update to the 21st century, *J. Coastal Res.*, *19*, 287–295.

Wright, W. R., and C. E. Parker (1976), A volumetric temperature/salinity census for the Middle Atlantic Bight, *Limnol. Oceanogr.*, *21*, 563–571.

Yin, J., M. E. Schlesinger, and R. J. Stouffer (2009), Model projections of rapid sea-level rise on the northeast coast of the United States, *Nat. Geosci.*, *2*, 262–266, doi:10.1038/NGEO462.

Zhang, W.G., G. G. Gawarkiewicz, D. J. McGillicuddy, and J. L. Wilkin (2011), Climatological mean circulation at the New England shelf break, *J. Phys. Oceanogr.*, *41*, 1874–1893.

Erratum

In the originally published version of this article, the affiliation for author M. Andres was incorrect. This error has since been corrected and this version may be considered the authoritative version of record.